# Chemical Mechanism of the Serine Acetyltransferase from *Haemophilus influenzae*†

Corey M. Johnson,‡ Bin Huang,§ Steven L. Roderick,§ and Paul F. Cook*,‡

*Department of Chemistry and Biochemistry, University of Oklahoma, 620 Parrington Oval, Norman, Oklahoma 73072, and Department of Biochemistry, Albert Einstein College of Medicine, Yeshiva University, 1300 Morris Park Avenue, Bronx, New York 10461*

*Received July 20, 2004; Revised Manuscript Received September 14, 2004*

ABSTRACT: The pH dependence of kinetic parameters was determined in both reaction directions to obtain information about the acid−base chemical mechanism of serine acetyltransferase from *Haemophilus influenzae* (*Hi*SAT). The maximum rates in both reaction directions, as well as the $V/K_{serine}$ and $V/K_{OAS}$, decrease at low pH, exhibiting a p$K$ of ∼7 for a single enzyme residue that must be unprotonated for optimum activity. The pH-independent values of $V_1/E_t$, $V_1/K_{serine}E_t$, $V/K_{AcCoA}E_t$, $V_2/E_t$, $V_2/K_{OAS}E_t$, and $V/K_{CoA}E_t$ are 3300 ± 180 $s^{-1}$, (9.6 ± 0.4) × $10^5$ $M^{-1}$ $s^{-1}$, 3.3 × $10^6$ $M^{-1}$ $s^{-1}$, 420 ± 50 $s^{-1}$, (2.1 ± 0.5) × $10^4$ $M^{-1}$ $s^{-1}$, and (4.2 ± 0.7) × $10^5$ $M^{-1}$ $s^{-1}$, respectively. The $K_i$ values for the competitive inhibitors glycine and L-cysteine are pH-independent. The solvent deuterium kinetic isotope effects on $V$ and $V/K$ in the direction of serine acetylation are 1.9 ± 0.2 and 2.5 ± 0.4, respectively, and the proton inventories are linear for both parameters. Data are consistent with a single proton in flight in the rate-limiting transition state. A general base catalytic mechanism is proposed for the serine acetyltransferase. Once acetyl-CoA and L-serine are bound, an enzymic general base accepts a proton from the L-serine side chain hydroxyl as it undergoes a nucleophilic attack on the carbonyl of acetyl-CoA. The same enzyme residue then functions as a general acid, donating a proton to the sulfur atom of CoASH as the tetrahedral intermediate collapses, generating the products OAS and CoASH. The rate-limiting step in the reaction at limiting L-serine levels is likely formation of the tetrahedral intermediate between serine and acetyl-CoA.

Serine acetyltransferase (SAT) catalyzes the regulated step in the *de novo* synthesis of L-cysteine in bacteria and plants, the transfer of an acetyl group from acetyl-CoA (AcCoA)[1] to the side chain hydroxyl of L-serine to give *O*-acetyl-L-serine (OAS) and CoASH. *O*-Acetylserine sulfhydrylase (OASS), a PLP-dependent enzyme, then catalyzes an elimination−addition reaction, in which the acetoxy group of the activated OAS is replaced with a thiol.

Serine acetyltransferase (EC 2.3.1.30) is a member of the hexapeptide acyltransferase family of enzymes. This family of proteins is composed of imperfect tandem repeated copies of a hexapeptide sequence (*1*). Three-dimensional structures of hexapeptide enzymes show that the hexapeptide sequence directs folding of a structural domain known as the left-handed parallel $\beta$-helix (L$\beta$H). Most enzymes in this family are known to catalyze acyl transfer utilizing the phosphopantothenoyl moiety of coenzyme A or the acyl carrier protein (*2*, *3*).

The kinetic mechanism of the SAT from *Haemophlius influenzae* (*Hi*SAT) has recently been determined (*4*). The *Hi*SAT catalyzes an ordered mechanism in which AcCoA is the first substrate bound followed by L-serine, and products are released with CoASH released last. At pH 6.5, the mechanism is equilibrium ordered, while it is steady state ordered at pH 7.5.

Little is presently known of the chemical mechanism of any of the hexapeptide enzyme family. In this paper, we use the pH dependence of the kinetic parameters and solvent deuterium kinetic isotope effects to probe the chemical mechanism of *Hi*SAT, a member of the hexapeptide family. A general base chemical mechanism with rate-limiting chemistry is proposed for *Hi*SAT.

## MATERIALS AND METHODS

*Chemicals.* L-Serine, OAS, glycine, DTNB, AcCoA, and coenzyme A were from Sigma. The buffers Mes, Tris, Hepes, Ches, Taps, and Bis-Tris were from Research Organics, Inc. Deuterium oxide was from Cambridge Isotope Laboratories, Inc. Monobasic and dibasic potassium phosphates were from EM Science. All other chemicals and reagents were obtained from commercial sources, were reagent grade, and were used without purification.

† This work was supported by a grant from the National Science Foundation to P.F.C. (MCB 0111024) and the Grayce B. Kerr endowment to the University of Oklahoma for the research of P.F.C., and a grant from the National Institutes of Health to S.L.R. (AI 42154).

* To whom correspondence should be addressed. E-mail: pcook@chemdept.chem.ou.edu. Telephone: (405) 325-4581. Fax: (405) 325-7182.

‡ University of Oklahoma.

§ Yeshiva University.

[1] Abbreviations: AcCoA, acetyl-CoA; CoA or CoASH, coenzyme A; OAS, *O*-acetyl-L-serine; OASS, *O*-acetylserine sulfhydrylase; *Hi*SAT, serine acetyltransferase from *H. influenzae*; L$\beta$H, left-handed parallel $\beta$-helix; DTNB, 5,5′-dithiobis(2-nitrobenzoic acid); BSA, bovine serum albumin; TNB, 5-thio-2-nitrobenzoate; Bis Tris, bis(2-hydroxyethyl)iminotris(hydroxymethyl)methane; Ches, 2-(*N*-cyclohexylamino)ethanesulfonic acid; Mes, 2-(*N*-morpholino)ethanesulfonic acid, monohydrate; Hepes, *N*-(2-hydroxymethyl)piperazine-*N*-2-ethanesulfonic acid; Taps, *N*-[tris(hydroxymethyl)methyl]-3-aminopropanesulfonic acid; Tris, tris(hydroxymethyl)aminomethane hydrochloride; DCl, deuterium chloride; KOD, potassium deuterioxide; $D_2O$, deuterium oxide.

10.1021/bi048450h CCC: $27.50 
Published on Web 11/17/2004

*Enzyme.* Serine acetyltransferase from *H. influenzae* was purified according to the method of ref *5* and maintained and stored frozen in 20 mM Tris (pH 7.5), 50 mM NaCl, and 0.02% (w/v) sodium azide. Enzyme dilutions (1.3 $\mu$g/mL) were prepared fresh in 50 mM Tris (pH 7.5), 15% glycerol, and 100 $\mu$g/mL BSA for use in assays. Control experiments were carried out to ensure no interference from BSA in the assays. The diluted enzyme is stable for several days under these conditions.

*Enzyme Assays.* In the direction of OAS formation, two assays for SAT were used. Reactions were carried out in cuvettes with a path length of 1 cm in a final volume of 0.4 mL containing the following 100 mM buffer, 0.45 mM DTNB, AcCoA (varied), L-serine (varied), and an appropriate amount of the enzyme. The buffer concentration was at times increased depending on the nature of the substrate and the concentration of substrate required for saturating conditions. The production of CoA was coupled to a disulfide exchange reaction with DTNB, and the appearance of TNB was monitored spectrophotometrically (*6*). Rates were calculated using an extinction coefficient of 13 600 $M^{-1}$ $cm^{-1}$ for TNB at 412 nm. For initial velocity measurements in the direction of AcCoA formation, the absorbance of the thioester bond was monitored spectrophotometrically at 232 nm ($\Delta\epsilon_{232}$ = 4500 $M^{-1}$ $cm^{-1}$) (*7*). Assays were carried out in 100 mM phosphate using a cuvette with a path length of 0.2 cm. Phosphate buffer was used to eliminate the absorbance of Mes or other buffers at 232 nm. Solutions of OAS were prepared fresh and adjusted to pH 6.5 where it is stable prior to the experiments. A unit of SAT is defined as the amount of enzyme required to produce 1 $\mu$mol of product in 1 min at pH 7.5 and 25 °C.

*pH Studies.* The initial velocity was measured at pH 7.5 as a function of AcCoA concentration and a fixed concentration of serine, and this was repeated at several different fixed concentrations of serine to generate an initial velocity pattern. The initial velocity pattern was then repeated at pH 6.5, 8.5, and 9.5 to determine kinetic parameters at the extremes of pH and to obtain information about the pH dependence of the kinetic mechanism (*4*). Initial rate data were then obtained as a function of pH by fixing one reactant at a saturating concentration (5$K_m$ for AcCoA) and varying the concentration of the other reactant. In this way, the pH dependences of $V_1$, $V_1/K_{serine}$, $V_1/K_{AcCoA}$, $V_2$, $V_2/K_{OAS}$, and $V_2/K_{CoA}$ were measured. The maximum rate in both reaction directions was obtained at pH 7 using the same enzyme stock solution varying substrate concentrations in a constant ratio and extrapolating to an infinite substrate concentration. All data were then normalized using the measured $V_{max}$ values. Profiles in the direction of CoA acetylation were only obtained from pH 5.5−8 due to the instability of OAS at high pH. The pH was measured before and after the reaction with changes limited to ≤0.1 pH unit. The pH was maintained using the following buffers at a concentration of 100 mM (or higher) in the direction of L-serine acetylation: pH 5.5−6.5 for Mes, pH 6.0 for Bis-Tris, pH 6.5−8.5 for Hepes, pH 7.5 for Tris, pH 8.5 for Taps, and pH 9.0−10.0 for Ches. In the direction of CoA acetylation, 100 mM phosphate was used from pH 5.5 to 8.

Data were also obtained for an inhibitor competitive with the substrate in the direction of L-serine acetylation. The dissociation constant for glycine (competitive vs L-serine) was measured at pH 6 and 8. The AcCoA concentration was fixed at 5$K_{AcCoA}$ and that of serine fixed at $K_{serine}$, and the initial rate was measured at different concentrations of glycine. Data were then analyzed as $1/v$ versus glycine with the abscissa intercept equal to $-2K_{i\ glycine}$.

*Proton Inventory Experiments and Solvent Deuterium Isotope Effects.* In the forward reaction direction, finite isotope effects were observed, and proton inventory experiments were carried out to more accurately measure the solvent deuterium kinetic isotope effect and estimate the number of protons in flight in the rate-determining transition state. Both the DTNB and 232 nm assays were utilized to measure $V_1$ and $V_1/K_{serine}$ at pH(D) 8.5 in 100% $H_2O$, 46% $D_2O$, and 96% $D_2O$. $V/K_{AcCoA}$ was also measured at pH(D) 7.5. In all cases, the pH(D) used to measure the isotope effect was above the p$K$ observed in the pH−rate profiles.

If a single proton is transferred in the rate-determining transition state, a plot of the rate constant versus atom fraction of deuterium ($n$) will be a linear. If more than one proton is transferred in a single transition state, the plot will be bowl-shaped (concave upward), while if protons are transferred in multiple transition states, the plot will be a dome-shaped plot (concave downward) (*8*).

*Data Processing.* Reciprocal initial velocities were plotted as a function of reciprocal substrate concentrations, and all plots were linear. Data were fitted using the appropriate rate equations and EnzFitter. Data for pH−rate profiles that exhibit a decrease with a limiting slope of 1 at low pH were fitted using eq 1. Data for $V$ and $V/K$ deuterium isotope effects were fitted using eq 2.

$$\log Y = \log\left(\frac{C}{1+\frac{H}{K_1}}\right) \quad (1)$$

$$v = \frac{VA}{K_a(1+F_iE_{V/K})+A(1+F_iE_V)} \quad (2)$$

In eq 1, $Y$ is the value of $V$ or $V/K$ at any pH, $C$ is the pH-independent value of $Y$, $H$ is the hydrogen ion concentration, and $K_1$ represents the acid dissociation constants for enzyme or substrate functional groups. In eq 2, $v$ is the initial velocity, $V$ is the maximum velocity, $A$ is the concentration of substrate A, $K_a$ is $K_m$ for the variable substrate, $F_i$ is the fraction of $D_2O$ in the solvent, and $E_{V/K}$ and $E_V$ are the isotope effects − 1 on $V/K$ and $V$, respectively. Proton inventories are linear, and the rate versus the percent $D_2O$ was fitted to the equation for a straight line.

## RESULTS

*pH Dependence of Kinetic Parameters for HiSAT.* The pH dependence of the kinetic parameters provides information about the protonation state of enzyme and/or reactant functional groups required for enzyme conformation, binding, and catalysis. To be certain the kinetic mechanism of the enzyme does not change with pH, select initial velocity patterns diagnostic for the proposed kinetic mechanism were obtained at the extremes of pH. Initial velocity patterns obtained for SAT in the direction of L-serine acetylation are consistent with an equilibrium ordered mechanism at pH 6.5, and the ordered mechanism is maintained at pH 7.5, but

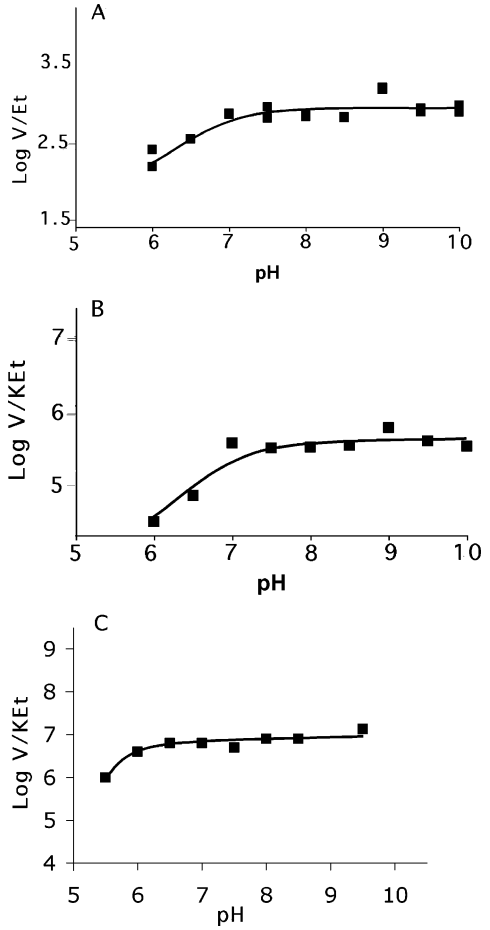


FIGURE 1: pH dependence of kinetic parameters in the direction of serine acetylation. pH−rate profile for $V_1$ (A), $V_1/K_{serine}$ (B), and $V/K_{AcCoA}$ (C). Points are experimental values, and curves are theoretical based on a fit to eq 1 for $V_1$ and $V_1/K_{serine}$. The curve for $V_1/K_{AcCoA}$ is drawn by eye, since data were not collected at a sufficiently low pH to give a meaningful fit to eq 1.

changes to steady state ordered (*4*). Initial velocity patterns obtained at pH extremes in the direction of CoA acetylation are consistent with a sequential kinetic mechanism in which CoA is the first substrate bound and OAS binds second (data not shown).

In the direction of L-serine acetylation, $V_1/E_t$ and $V_1/K_{serine}E_t$ decrease at low pH, giving a limiting slope of 1 and a single p$K$ of ~7 (Figure 1). L-Serine has no p$K$ values over the pH range that was studied, and the p$K$ exhibited in the pH−rate profiles likely reflects an enzyme side chain important in catalysis. On the other hand, $V_1/K_{AcCoA}E_t$ decreases at low pH, giving a p$K$ of ~6. Because of enzyme stability, it is difficult to collect data below pH 5.5. Since AcCoA is the first reactant bound, the pH dependence reflects groups required for binding of AcCoA. Estimates of the pH-independent values of the kinetic parameters are summarized in Table 1.

In the reverse reaction direction, $V_2/E_t$ and $V_2/K_{OAS}E_t$ decrease at low pH with limiting slopes of +1, giving p$K$ values of 6.1 and 7, while the $V_2/K_{CoA}E_t$ pH profile decreases below a p$K$ of 6.4 with a limiting slope of 1 (Figure 2). As observed in the forward reaction direction, the p$K$ observed in the $V$ and $V/K_{OAS}$ profiles reflects a catalytic group, while

Table 1: Summary of pH Data

| parameter | p$K$ ± standard error | $C^a$ ± standard error |
|---|---|---|
| $V_1$ ($s^{-1}$) | 6.8 ± 0.2 | 3300 ± 350 |
| $V/K_{serine}$ ($M^{-1}$ $s^{-1}$) | 7.2 ± 0.2 | (9.6 ± 0.4) × $10^5$ |
| $V/K_{AcCoA}$ ($M^{-1}$ $s^{-1}$) | 6 | 3.3 × $10^6$ |
| $V_2$ ($s^{-1}$) | 6.1 ± 0.1 | 420 ± 50 |
| $V/K_{OAS}$ ($M^{-1}$ $s^{-1}$) | 7.0 ± 0.2 | (2.1 ± 0.5) × $10^4$ |
| $V/K_{CoA}$ ($M^{-1}$ $s^{-1}$) | 6.4 ± 0.2 | (4.2 ± 0.7) × $10^5$ |

[a] $C$ is the pH(D)-independent value of the parameter. All parameters are divided by $E_t$.

that observed in the $V/K_{CoA}$ profile likely reflects an enzyme group important for binding CoA. Estimates of the pH-independent values of the kinetic parameters are summarized in Table 1.

*pH Dependence of the $K_i$ for Glycine.* Glycine was utilized as a dead-end inhibitor. At pH 6 and 8, estimated $K_i$ values for glycine are 36 and 55 mM, respectively, and are pH-independent within error. Data are consistent with the pH independence of $K_{serine}$ and, thus, the pH independence of amino acid binding (see below) over the pH range that was studied.

*Solvent Deuterium Kinetic Isotope Effects and Proton Inventory Experiments.* The pH−rate profiles for all kinetic parameters are pH-independent at pH ≥7.5 (Figure 1). The solvent deuterium isotope effect studies were carried out above the p$K$ value to prevent interference from the equilibrium isotope effect on the acid dissociation constant of the group(s) titrated in the pH−rate profiles.

Values of $V_1$ and $V_1/K_{serine}$ were measured as a function of the percentage of $D_2O$ in solution (Figure 3). An estimate of the solvent kinetic isotope effects was obtained from a fit of the data to eq 3. Values of $^{D_2O}V$ and $^{D_2O}(V/K_{serine})$ are 1.9 ± 0.1 and 2.5 ± 0.4, respectively. Replots of $V_1/K_{serine}$ and $V_1$ versus the percent $D_2O$ are linear, indicating a single proton in flight in the rate-determining transition state (*8*). In a separate experiment, a value of 1 was measured for $^{D_2O}(V_1/K_{AcCoA})$ (data not shown).

## DISCUSSION

*Proton Inventory and Kinetic Mechanism.* The SKIEs on $V$ and $V/K_{serine}$ are ~1.9 and ~2.5, respectively. The proton inventories are linear, indicating a single proton in flight in the rate-determining step of the reaction (*8*). The step in which the proton is transferred is likely the chemical step once the E:serine:AcCoA complex is formed as indicated by the large isotope effects on $V/K$. Thus, the nucleophilic attack by the serine hydroxyl is likely limiting, with a general base accepting a proton in this reaction.

The difference in value of the $V/K_{serine}$ and $V$ isotope effects shows that the steps accompanying proton transfer are not solely rate-limiting under $V$ conditions. The isotope effect on $V/K_{serine}$ represents the reaction from the binding of the substrate, serine, until the release of the first product, OAS. The $V$ profile represents the reaction with both products bound, and includes all steps to the release of both products and re-formation of the free enzyme. The values of 2.5 and 1.9 for the $V/K$ and $V$ solvent deuterium kinetic isotope effects, respectively, show that some step contained only in $V$ also contributes to rate limitation (i.e., release of the last product). The observed value of 2.5 on $^{D_2O}(V/K_{serine})$ is likely

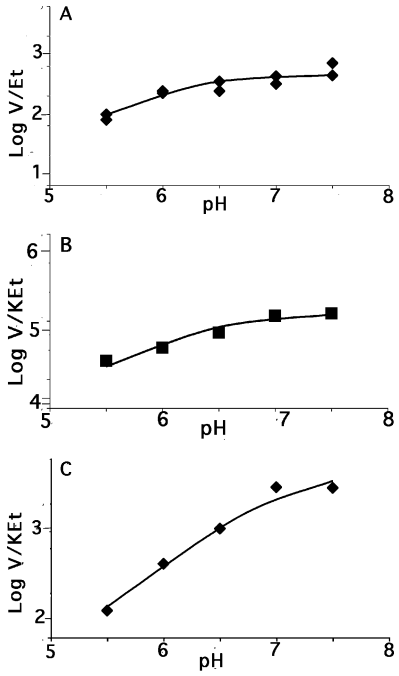


FIGURE 2: pH dependence of kinetic parameters in the direction of CoA acetylation. pH−rate profile for $V_2$ (A), $V_2/K_{OAS}$ (B), and $V/K_{CoA}$ (C). Points are experimental values, and curves are theoretical based on a fit to eq 1.

the intrinsic value given the magnitude of the effect. On this basis, an estimate of the relative rate of CoA release compared to the chemical step can be obtained. (Data also suggest that chemistry limits with serine limiting, and thus, $K_{serine}$ is equal to the $K_d$ for serine from the E−AcCoA−serine complex.) The mechanism for SAT is shown schematically below at saturating reactant concentrations (Scheme 1).

Scheme 1

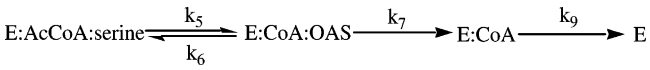


The equation for the solvent deuterium kinetic isotope effect on $K_{eq}$ as represented by the scheme is shown in eq 3. The equations for $V$ and the solvent deuterium kinetic isotope effects on $V$ are shown in eqs 4 and 5.

$$^{D_2O}K_{eq} = \frac{^{D_2O}k_5}{^{D_2O}k_6} \quad (3)$$

$$V = \frac{k_5}{1 + k_5\left(\frac{1}{k_7} + \frac{1}{k_9}\right) + \frac{k_6}{k_7}} \quad (4)$$

$$^{D_2O}V = \frac{^{D_2O}k_5 + k_5\left(\frac{1}{k_7} + \frac{1}{k_9}\right) + {}^{D_2O}K_{eq}\left(\frac{k_6}{k_7}\right)}{1 + k_5\left(\frac{1}{k_7} + \frac{1}{k_9}\right) + \frac{k_6}{k_7}} \quad (5)$$

The values of $K_{OAS}$ (24 mM) and $K_{iOAS}$ as a product inhibitor (80 mM) (*4*) are very high, suggesting rapid release of OAS. The relative values of $V_1$ and $V_2$ are within a factor of 8, suggesting $k_7 > k_5$ and $k_6$ and eq 5 reduces to eq 6.

$$^{D_2O}V = \frac{^{D_2O}k_5 + \frac{k_5}{k_9}}{1 + \frac{k_5}{k_9}} \quad (6)$$

Substituting values of 1.9 for $^{D_2O}V$ and 2.5 for $^{D_2O}k_5$ gives a value of 0.67 for $k_5/k_9$. Thus, the rate of release of CoA is only ~1.5 times greater than the rate of the chemical step. In agreement, the p$K$ observed in the $V_1/E_t$ pH−rate profile is perturbed slightly to low pH compared to $V_1/K_{ser}E_t$ (6.8 compared to 7.2).

*Interpretation of the pH Dependence of Kinetic Parameters.* The $V/K$ for a reactant is obtained at a limiting concentration of one of the reactants and saturating levels of all others. $V$ is obtained at saturating concentrations of substrate, and the enzyme form that builds up in the steady state predominates. The pH dependence of $V/K$ thus reflects the protonation state of group(s) on the free enzyme and/or reactant responsible in a given protonation state for binding and/or catalysis, while the pH dependence of $V$ reflects groups on enzyme required for catalysis. The determination of an ordered mechanism for *Hi*SAT (*4*) allows the pH profiles to be interpreted in terms of enzyme forms or species that predominate under given conditions. The free enzyme and AcCoA predominate for the $V/K_{AcCoA}$ profile, the E:AcCoA enzyme form and serine predominate for the $V/K_{serine}$ profile, and central complexes (primarily E:AcCoA:serine complex; see above) predominate for the $V_1$ profile. In the reverse reaction direction, E and CoA predominate for $V/K_{CoA}$, the E:CoA complex and OAS predominate for $V/K_{OAS}$, and central complexes (primarily E:CoA:OAS; see above) predominate for $V_2$.

The $V/K_{AcCoA}$ decreases at low pH, giving a p$K$ of ~6 necessary for binding the acetyl donor. The crystal structure of HiSAT has been determined with CoA bound to the active site (*5*). According to the structure, the carbonyl groups of the cofactor pantothenyl arm are hydrogen bonded to the backbone NHs of A200(A) and A218(A) (A and B in parentheses indicate the residues are contributed by different subunits). Hydrogen bonds are also accepted by the peptide oxygens of G180(B) and T181(B) from the two amide nitrogen groups in the pantothenyl arm of the cofactor. These hydrogen bonds stabilize an extended conformation of the cofactor and direct its thiol toward H154(A) and Q174(A). K215(A), T231(A), and R238(B) are residues with side chains located near the AMP end of the CoA that participate in binding the cofactor (*5*). None of the ionizable residues that interact with CoA directly are likely to have p$K$ values near 6. The identity of the group may be the 2′-phosphate of the AMP portion of the cofactor. This aspect will have to await further study.

The SAT has an ordered kinetic mechanism with serine adding to the E:AcCoA complex and OAS adding to the E:CoA complex (*4*). Thus, $V_1/K_{serine}$ includes steps from addition of serine to release of OAS, and $V_2/K_{OAS}$ includes steps from addition of OAS to release of serine. The $V_1/K_{serine}$ and $V_2/K_{OAS}$ pH−rate profiles decrease at low pH below a single p$K$ value of ~7. Since a single p$K$ is observed

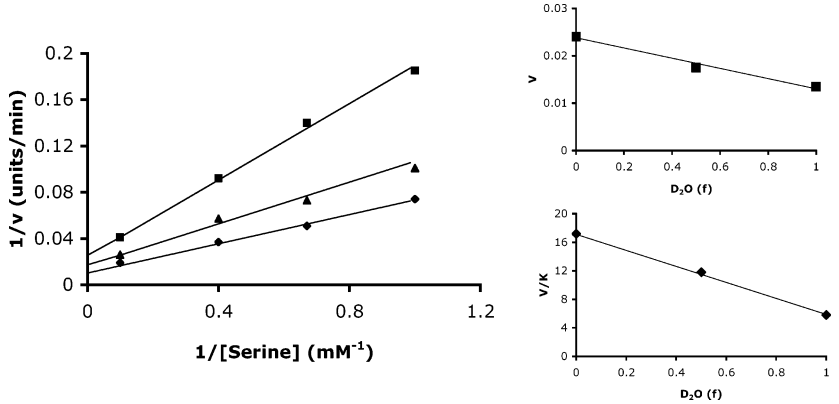


FIGURE 3: Proton inventory results. $V_1$ and $V/K_{serine}$ were measured at the pH(D)-independent value of 8.5 in 100% $H_2O$ (◆), 46% $D_2O$ (▲), and 96% $D_2O$ (■). Points are experimental values, and curves are theoretical based on a fit to eq 2. The insets show the linear dependence of $V$ and $V/K$ on percent $D_2O$.

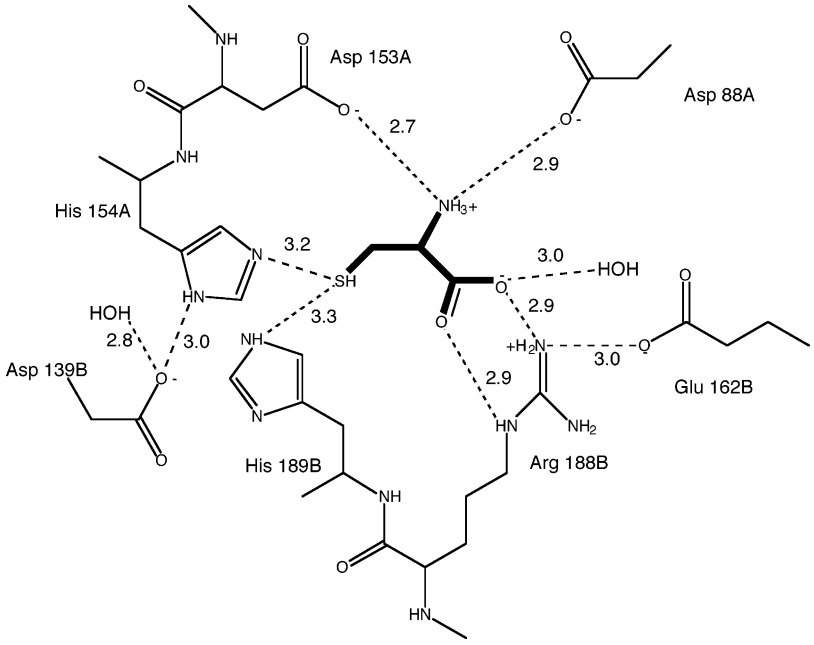


FIGURE 4: Schematic of the active site of serine acetyltransferase from *H. influenzae* with cysteine bound to the serine-binding site. Cysteine is tightly bound by all functional groups. Asp88(A) and Asp153(A) interact with the α-amine, while Arg188(B) donates two hydrogen bonds to the carboxylate. The side chain thiol interacts with His154(A) and His189(B), and Asp139(B) is in dyad linkage with His154(A).

in both pH−rate profiles, data suggest a single residue that acts as a general base in both reaction directions. The identity of the p$K$ value in both reaction directions, i.e., in the E:AcCoA and E:CoA complexes, suggests no environmental perturbation of the p$K$ by the acetyl moiety of AcCoA.

The p$K$ values estimated from the $V_1$ and $V_2$ pH−rate profiles differ by almost a pH unit, suggesting release of AcCoA contributes to rate limitation in the reverse reaction direction. Although the back reaction is slower by a factor of 8 than the forward reaction, it is still quite fast with a turnover number of 400 $s^{-1}$. It is not unreasonable that release of the last product could limit the overall rate of CoA acetylation.

On the basis of the acid−base chemistry required in the acetyl transfer reaction, the group with a p$K$ of 7 is believed to represent a general base required to accept a proton from the serine hydroxyl in the acetyl transfer reaction. In the reverse reaction direction, the same group must be unprotonated to accept a proton from CoA. When the p$K$ values in $V_1/K_{serine}$ and $V_1$ pH−rate profiles are compared, the same group is observed with little perturbation. Therefore, serine binds with equal affinity to the protonated and unprotonated enzyme (*9*). In agreement, no pH dependence was observed for the $K_i$ value of glycine.

*Chemical Mechanism.* The pH−rate profiles and solvent isotope effects allow a chemical mechanism to be proposed as shown in Scheme 2. The single group observed in both reaction directions suggests general base catalysis by a single enzyme residue. Once both substrates are bound, the reaction sequence is proposed to begin by nucleophilic attack of the oxygen from the serine side chain hydroxyl on the carbonyl carbon of AcCoA (I in Scheme 2). The general base accepts the proton from the side chain hydroxyl as it attacks the carbonyl of AcCoA. The carbonyl oxygen is likely stabilized by positive dipoles from backbone nitrogens (*5*). The nucleophilic attack of the serine oxygen on the AcCoA carbonyl results in a tetrahedral intermediate (II). The same residue that served as a general base in the formation of the tetrahedral intermediate then acts as a general acid and donates a proton to the sulfur atom of CoA (II in Scheme 2) either as the tetrahedral intermediate collapses or after a thiolate is expelled, giving products OAS and CoA (III in

Scheme 2

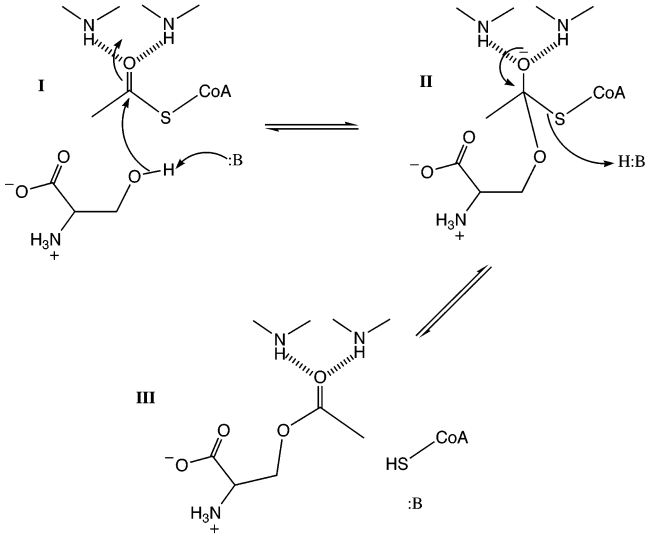


Scheme 2). The solvent isotope effect studies support the proposed general base mechanism. The single proton in flight in the transition state, as identified by the proton inventory experiments, is likely the one accepted by the general base from the serine side chain hydroxyl.

The identity of the general base catalytic residue has not been determined. A structure of *Hi*SAT has recently been published showing L-cysteine bound to the active site and occupying what appears to be the serine-binding site. Several potential general base residues in the active site in the E−cysteine complex are shown (*5*) (Figure 4). H154(A) and H189(B), which are located on either side of and within hydrogen bonding distance of the cysteine thiol, are likely candidates. A catalytic dyad is formed between H154(A) and D139(B), making it the most likely candidate. The identity of the general base is currently under investigation via site-directed mutagenesis studies of these and other active site residues.

*Comparison with Other Enzymes.* SAT is a member of the hexapeptide acyltransferase family of enzymes in which a six-amino acid residue motif directs folding of a structural domain known as the left-handed $\beta$-helix (L$\beta$H) (*1*). All of the known hexapeptide acyltransferases have similar active site locations and patterns of interaction (*10*). All of the mechanistic work carried out to date for this enzyme family shows similar sequential kinetic mechanisms (*10*−*13*). Similar hexapeptide proteins such as uridyl diphosphate-*N*-acetylglucosamine 3-*O*-acyltransferase, the xenobiotic acetyltransferase from *Pseudomonas aeruginosa* (*Pa*XAT), and Vat(D), a streptogramin acetyltransferase, all have histidines identified as important catalytic residues (*10*, *14*, *15*), all of which are in dyad linkage with a negative charge or a negative dipole.

Even non-hexapeptide proteins that catalyze similar acetyl transfer reactions such as chloramphenicol acetyltransferase and carnitine acetyltransferase do so by general base catalysis via a putative catalytic histidine residue. In the case of carnitine acetyltransferase, the histidine is part of a catalytic Glu-His dyad (*16*, *17*). Additional work is clearly necessary to identify common structural and mechanistic modalities within this diverse enzyme class.

## REFERENCES


1. Vaara, M. (1992) Eight bacterial proteins, including UDP-*N*-acetylglucosamine acyltransferase (LpxA) and three other transferases of *Escherichia coli*, consist of a six-residue periodicity theme, *FEMS Microbiol. Lett. 97*, 249−254.
2. Downie, J. A. (1989) The *nodL* gene from *Rhizobium leguminasarum* is homologous to the acetyltransferase encoded by *lacA* and *cysE*, *Mol. Microbiol. 3*, 1649−1651.
3. Anderson, M. S., and Raetz, C. R. H. (1987) Biosynthesis of lipid A precursors in *Escherichia coli*. A cytoplasmic acyltransferase that converts UDP-*N*-acetylglucosamine to UDP-3-O-(R-3-hydroxymyristoyl)-*N*-acetylglucosamine, *J. Biol. Chem. 262*, 5159−5169.
4. Johnson, C. M., Huang, B., Roderick, S. L., and Cook, P. F. (2004) Kinetic Mechanism of Serine Acetyltransferase from *Haemophilus influenzae*, *Arch. Biochem. Biophys. 429*, 115−122.
5. Olsen, L. R., Huang, B., Vetting, M. W., and Roderick, S. L. (2004) Structure of serine acetyltransferase in complexes with CoA and its cysteine feedback inhibitor, *Biochemistry 43*, 6013−6019.
6. Cook, P. F., and Wedding, R. T. (1977) Cysteine synthetase from *Salmonella typhimurium* LT-2. Aggregation, kinetic behavior, and effect of modifiers. *J. Biol. Chem. 253*, 7874−7879.
7. Leu, L., and Cook, P. F. (1994) Kinetic mechanism of serine transacetylase from *Salmonella typhimurium*, *Biochemistry 33*, 2667−2671.
8. Quinn, D. M., and Sutton, L. D. (1991) in *Enzyme Mechanism from Isotope Effects*, pp 73−126, CRC Press, Boca Raton, FL.
9. Cleland, W. W. (1979) Statistical analysis of enzyme kinetic data, *Methods Enzymol. 63*, 103−138.
10. Sugantino, M., and Roderick, S. L. (2002) Crystal structure of Vat(D): an acetyltransferase that inactivates streptogramin group A antibiotics, *Biochemistry 41*, 2209−2216.
11. Olsen, L. R., and Roderick, S. L. (2001) Structure of the *Escherichia coli* GlmU pyrophosphorylase and acetyltransferase active sites, *Biochemistry 40*, 1913−1921.
12. Beaman, T. W., Sugantino, M., and Roderick, S. L. (1998) Structure of the hexapeptide xenobiotic acetyltransferase from *Pseudomonas aeruginosa*, *Biochemistry 37*, 6689−6696.
13. Hirvas, L., Koski, P., and Vaara, M. (1990) Primary structure and expression of the Ssc-protein, *Biochem. Biophys. Res. Commun. 173*, 53−59.
14. Murray, I. A., and Shaw, W. V. (1997) O-Acetyltransferases for chloramphenicol and other natural products, *Antimicrob. Agents Chemother. 41*, 1−6.
15. Wyckoff, T., and Raetz, C. R. H. (1999) The active site of *Escherichia coli* UDP-*N*-acetylglucosamine acyltransferase. Chemical modification and site-directed mutagenesis, *J. Biol. Chem. 274*, 27047−27055.
16. Kleanthous, C., Cullis, P. M., and Shaw, W. V. (1985) 3-(Bromoacetyl)chloramphenicol, an active site directed inhibitor for chloramphenicol acetyltransferase, *Biochemistry 24*, 5307−5313.
17. Wu, D., Govindasamy, L., Lian, W., Gu, Y., Kukar, T., Agbandje-McKenna, M., and McKenna, R. (2003) Structure of human carnitine acetyltransferase. Molecular basis for fatty acyl transfer, *J. Biol. Chem. 278*, 13159−13165.


BI048450H